Effectiveness of recycled rubber aggregate in ASR mitigation of cement-based composites

Materials and Structures (2026) 59:297
https://doi.org/10.1617/s11527-026-03186-2

ORIGINAL ARTICLE

Effectiveness of recycled rubber aggregate in ASR mitigation of cement-based composites

By Daria Jóźwiak-Niedźwiedzka · Dominik Nowicki · Piotr Denis · Magdalena Osial · Alessandro P. Fantilli

Received: 26 February 2026 / Revised: 15 April 2026 / Accepted: 30 June 2026 / Published online: 7 July 2026

Abstract Rubber derived from end-of-life tires offers a sustainable solution for reducing the environmental impact of cement-based materials. In this study, recycled rubber aggregate (RRA) was used as a partial volumetric replacement (15% and 30%) of natural fine sand in cement-based mortars to evaluate its effectiveness in mitigating alkali–silica reaction (ASR). The experimental program included mechanical testing, ASR expansion measurements, and microstructural analyses. The results showed that increasing RRA content led to a reduction in compressive strength by up to 24.1% and flexural strength by up to 19.8% after 28 days of curing. Despite this reduction, a significant improvement in ASR resistance was observed. For mortars containing highly reactive aggregates, ASR expansion decreased from approximately 0.73% in the reference mixture to 0.47% with 30% RRA, corresponding to a reduction of up to 33%. Microstructural observations confirmed that RRA acts as a stress-relieving inclusion, limiting crack propagation and reducing ASR gel formation. Physicochemical analyses (XRD, TGA, and FTIR) indicated that alkaline treatment induces surface oxidation of RRA without affecting the stability of mineral components. The findings demonstrate that ASR mitigation is not solely due to dilution of reactive aggregates, but also to the elastic and microstructural buffering effects of RRA. Furthermore, a simple predictive model is proposed to estimate the required rubber content for effective ASR mitigation.

Keywords Recycled rubber aggregate · Reactive aggregate · Flexural test · Compression tests · Microstructural analyses

B. D. Jóźwiak-Niedźwiedzka (✉) · D. Nowicki · P. Denis · M. Osial
Institute of Fundamental Technological Research, Polish Academy of Sciences, Pawińskiego 5B, 02-106 Warsaw, Poland
e-mail: djozwiak@ippt.pan.pl

D. Nowicki
e-mail: dnowicki@ippt.pan.pl

P. Denis
e-mail: pdenis@ippt.pan.pl

M. Osial
e-mail: mosial@ippt.pan.pl

A. Fantilli
Dept. of Structural, Building, and Geotechnical Engineering - DISEG, Politecnico di Torino, Corso Duca Degli Abruzzi 24, 10129 Torino, Italy
e-mail: alessandro.fantilli@polito.it

1 Introduction

The management of end-of-life materials, including persistent non-biodegradable used tires, represents a significant challenge to global sustainability goals. Waste tire rubber constitutes a major part of this problem, as over one billion waste tires are generated annually worldwide [1]. Data from the U.S. Tire Manufacturers Association [2] indicate that the

United States produces more than 230 million scrap tires annually, with about 75 million stockpiled. In Europe, the European Association of Tire and Rubber Producers [3] reported that 4.2 million tons of end-of-life tires were disposed in 2023, of which 93% were recovered through reuse, recycling, or energy production [4]. However, improper disposal methods such as landfilling, open burning, and illegal dumping remain widespread, causing serious environmental and health risks [5].

At the same time, end-of-life tires are increasingly recognized as a potential source of secondary raw materials, because recycling rubber reduces non-renewable energy consumption and greenhouse gas emissions [6]. Indeed, substituting 10–30% of natural sand with crumb rubber decreases the demand for virgin aggregate and lowers the energy intensity of quarrying, crushing, and transportation. Bravo and de Brito [4] estimated that aggregate extraction and processing contribute approximately 50–100 kg CO_2 per ton of concrete, implying that partial replacement with recycled rubber may reduce emissions by 5–15%. Moreover, Shu and Huang [7] emphasized that valorisation of end-of-life tires avoids incineration or landfilling, thereby preventing additional greenhouse gas emissions. Recent life cycle assessment studies [8, 9] confirm that in rubberized concretes a consistent reduction in embodied carbon compared with conventional mixtures can be achieved, particularly when high substitution levels of non-renewable aggregates are implemented.

A promising and sustainable strategy is therefore the incorporation, within cement-based composites, of recycled rubber aggregate (RRA), typically obtained from end-of-life tires via mechanical or cryogenic processing, producing crumb rubber or shreds of various sizes. Shu and Huang [7] highlighted the potential of rubberized concrete to balance sustainability and performance, while Muñoz-Sánchez et al. [5] explored how construction materials can innovate by using waste rubber. These materials can partially replace cement [9] or natural aggregates [5, 8], reducing the demand for virgin resources and creating a recycling pathway for waste tires.

Previous studies [1, 4, 5] showed that rubber incorporation modifies density, workability, and overall behaviour of cementitious composites, opening opportunities for specialized applications. Also, the mechanical performance of rubberized composites has been widely studied. In general, rubber addition reduces compressive strength due to a lower stiffness of rubber with respect to mineral aggregates [10, 11], but enhances ductility, toughness, and impact resistance [12–14].

Ling et al. [15] reported improved energy absorption capacity, which increases resilience to dynamic loading, whereas Turatsinze et al. [12] showed that rubberized mortars exhibit superior post-cracking behaviour and strain capacity. Zhang et al. [16] further confirmed that ultra-high-performance concrete with crumb rubber powders displays enhanced dynamic compressive behaviour, highlighting the role of rubber in improving toughness and energy dissipation under impact. Microstructural studies also highlight the importance of the interfacial transition zone (ITZ) between rubber particles and the cement matrix [17], ITZ in rubberized concrete is weaker than in conventional composites, but the flexibility of rubber can enhance toughness and energy absorption. The porous structure of rubber aggregates may also influence water permeability and shrinkage, and age-related ITZ modifications indicate possible long-term stabilization of properties [17].

Research activities also focus on durability aspects, particularly alkali–silica reaction (ASR). Afshinnia and Poursaee [18] found that RRA mitigates ASR-related cracking, as rubber tends to absorb stress concentrations. Similarly, Abbas et al. [19] reported promising results regarding ASR mitigation when rubber aggregate substitutes stone sand. Nevertheless, from all the previous studies, it remains unclear whether reduced ASR expansion results from dilution of reactive sand or from the buffering effect of RRA against ASR-related stresses. To settle this issue, a new study, which examines the potential of recycled rubber aggregate to partially substitute natural expansive sand in cement-based mortars, is proposed herein. More precisely, mechanical performance, ASR mitigation, and microstructural development are analysed, with a focus on the behaviour of untreated and surface-treated RRA. By developing and validating a procedure for substituting natural sand with recycled rubber aggregate, not only a method to mitigate ASR expansion is introduced, but also the circular use of end-of-life tires is promoted. As a consequence, the reliance of concrete on virgin raw materials is remarkably reduced.

2 Materials

Ordinary Portland Cement (CEM I 52.5 R), characterized by a high alkali content ($Na_2O_{eq} = 0.87\%$) and a Blaine specific surface area of 546 $m^2 \cdot kg^{-1}$ was used in the study. It met standard requirements for soundness and strength development, making it suitable for testing purposes.

Three sands were used in this study (S1, S2, and S3), already investigated in other research projects [20].Two sands, S1 and S2, had different gradations (see Fig. 1): S1 sand was classified as moderately reactive (14-day expansion > 0.1% and ≤ 0.3%), corresponding to Class R1; S2 sand was classified as very highly reactive (14-day expansion > 0.45%), corresponding to Class R3, according to AASHTO R 80–17 [21]. The alkali reactivity was attributed mainly to the presence of microcrystalline and cryptocrystalline quartz, which are highly susceptible to alkali–silica reaction.

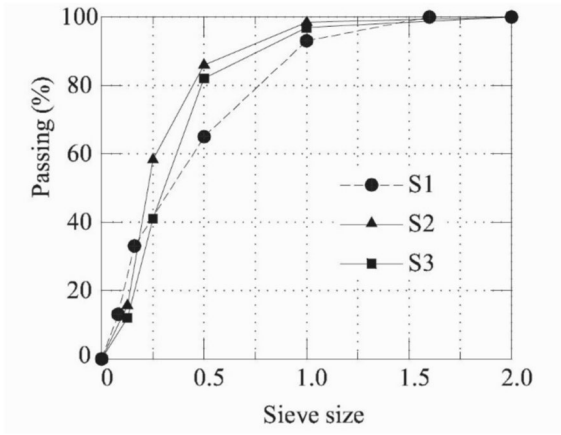

Fig. 1 Sieve curves of the analyzed sands

In addition to these reactive sands, a non-reactive quartz sand S3 (14-day expansion < 0.10%) was also taken into account for comparative purposes.

The physical properties of the sands, characterized by bulk density within the range of 1550–1650 kg/m^3, water absorption below 1.5%, and fineness modulus values between 1.6 and 2.2, were typical of fine natural aggregates [20].

The recycled rubber granulates used for this study was a dry, free flowing granulate with particle sizes ranging from 0.50 mm to 1.00 mm, characterized by irregularly shaped grains and a black colour. The bulk density was approximately 1200 kg m^{-3}. Both S1 and S2 sands were modified by partially substituting the sand fraction with recycled rubber granulate. Specifically, 15% and 30% of the sand masses retained on the 0.5 mm sieve was removed from S1 and S2 and replaced with an equal volume of rubber granulate, having a matching nominal particle size of 0.5 mm. This volumetric substitution preserved the original packing density and gradation of the sands.

In total, six sands were prepared to cast six mortars following the EN 196–1 [22] standard. The composition of these M mortars, used for the mechanical tests, are reported in Table 1. Reference mortars (S1-M-0 and S2-M-0) were prepared without rubber by using standard proportions of cement, sand, and water. For mortars incorporating recycled rubber aggregate, 15% (S1-M-15) or 30% (S1-M-30) of the sand S1 was replaced with recycled rubber (fraction at 0.50 mm), and the same amount of sand S2 was substituted by rubber granulate (S2-M-15 and S2-M-30). In addition, 30% of the mass of the highly reactive S2 sand was replaced with non-reactive sand S3 (mortar S2-M-30_S3). This substitution was introduced to evaluate whether the mitigation of ASR in rubberized mortars is solely a result of reducing the amount of reactive aggregate (i.e., dilution effect), or the recycled rubber aggregate provides an additional

Table 1 Composition (in kg/m^3) of the M mortars used for mechanical tests

Constituent	S1-M-0	S1-M-15	S1-M-30	S2-M-0	S2-M-15	S2-M-30	S2-M-30_S3
Cement	450	450	450	450	450	450	450
Sand S1	1350	1147	946	0	0	0	0
Sand S2	0	0	0	1350	1147	946	946
Sand S3	0	0	0	0	0	0	404
Water	225	225	225	225	225	225	225
RRA	0	50	100	0	50	100	0

beneficial mechanism, such as microstructural buffering or stress absorption. In other words, by including the mixture S2-M-30_S3, 30% of the expansive sand S2 sand was replaced with inert sand S3 instead of RRA, in order to determine whether or not RRA contributes as only a passive filler in suppressing ASR-induced expansion.

To evaluate the influence of recycled rubber aggregate on the expansion due to alkali–silica reaction, seven mortar mixtures were specifically prepared and tailored according to the AMBT protocol [23]. These A mortars were designed to mirror those reported in Table 1 and used in the mechanical test series. As shown in Table 2, A mortars were composed by the same reactive or moderately reactive sand types (S1 and S2), with 15% or 30% of the sand mass replaced by RRA. Similarly, to M mortars, the substitution was done volumetrically, preserving the particle size distribution by replacing the sand fractions with rubber granules of the same nominal size. The main tailoring difference between the mortars A and M was the w/c ratio, which was slightly reduced from 0.50 to 0.47 in the A mortars, according to the RILEM AAR-2 protocol [23]. Hence, a direct comparison between mechanical performance and durability behaviour under aggressive alkaline conditions was possible for companion mortars of Tables 1 and 2.

3 Methods

To evaluate the effects on recycled rubber aggregate resulting from alkaline exposure, a series of analytical tests were performed on RRA particles with a grain size varying from 0.50 mm to 1.00 mm (i.e., the fraction passing the sieve of 1 mm and retained at that of 0.5 mm). The aim was to understand how sodium hydroxide treatment may affect surface properties, thermal stability, and chemical composition of rubber, which in turn affects the behaviour of A mortars in terms of ASR mitigation and interfacial bond of RRA with the cement matrix.

Hence, 100 g of rubber granulate was suspended in 300 mL of 1 M NaOH solution for 30 min at room temperature. Afterwards, the specimens were dried under two conditions: air-dried at 20 °C and oven-dried at 80 °C, both for 24 h. After drying, the treated RRA was filtered and prepared for analysis.

Three complementary characterization methods were applied, X-ray Diffraction (XRD), Thermogravimetric Analysis (TGA), and Attenuated Total Reflectance Fourier-Transform Infrared Spectroscopy (ATR-FTIR). XRD analysis was performed using a Bruker D8 DISCOVER diffractometer (Cu anode, 40 kV, 40 mA), scanning in the 2θ range of 5°–65°, with a step size of 0.02° and 1 s per step. Phase identification was carried out using Diffrac.Eva software. TGA measurements were conducted from room temperature to 800 °C, at a heating rate of 10 °C/min under a nitrogen atmosphere (40 mL/min), using Perkin Elmer TGA 800 equipment. The aim was to determine the degradation profile of the polymeric matrix and assess whether NaOH treatment affected thermal stability.

The ATR-FTIR spectra were recorded in the 400–4000 cm^{-1} range using a Spectrum Two instrument. Before the analysis, the specimens were finely ground to improve spectral resolution. This test helped detect signs of surface oxidation, such as the appearance of hydroxyl groups or changes in hydrocarbon chains, which may influence adhesion to the cement matrix.

The evaluation of compressive and flexural strength of the M mortars (Table 1) was conducted in accordance with the EN 196-1 [22] standard. Three specimens, measuring $40 \times 40 \times 160$ mm^3, were prepared for each mortar mixture. The specimens were stored at 20 ± 1 °C with a relative humidity $\geq 90\%$ for

Table 2 Composition (in kg/m^3) of the A mortars used for ASR test

Constituent	S1-A-0	S1-A-15	S1-A-30	S2-A-0	S2-A-15	S2-A-30	S2-A-30_S3
Cement	440	440	440	440	440	440	440
Sand S1	990	842	693	0	0	0	0
Sand S2	0	0	0	990	842	693	693
Sand S3	0	0	0	0	0	0	297
Water	206.8	206.8	206.8	206.8	206.8	206.8	206.8
RRA	0	37	73	0	37	73	0

24 h under tightly fitted covers. Following demoulding, the specimens were immersed in water at 20 ± 1 °C until testing. Flexural strength was obtained from a three-point bending test, in which the load was applied at the midpoint of the prism up to the failure. After tested in bending, the two fractured halves of the prism were used to measure compressive strength, starting from the maximum load applied on the bearing surface. Both the tests were performed after 28 days of curing.

To evaluate the ASR potential of the aggregates and assess the mitigating effects of recycled rubber aggregate, the A mortars of Table 2 were subjected to AMBT [23]. This laboratory test preserves the natural characteristics of aggregates and ensures results similar to those observed on field, while adhering to specific test protocol. Three bars ($25 \times 25 \times 285$ mm^3) were prepared, initially cured for 24 h at room temperature, and then immersed in water at 80 °C for an additional 24 h. Following curing, the bars were submerged in a 1 M NaOH solution and maintained at 80 °C. To observe longer expansion, length measurements were taken starting from the 4th day till the 28th day after exposure.

After the expansion tests, fragments were extracted from the beams and analysed with a Scanning Electron Microscopy (SEM). They were dried at 50 °C for three days and impregnated with a low-viscosity epoxy resin to stabilize the microstructure. Subsequently, they were ground and polished with diamond pastes to create a smooth surface suitable for SEM. The polished specimens were coated with carbon to ensure electrical conductivity. SEM analysis was performed at an accelerating voltage of 15–20 kV using backscattered electron imaging (BSE) to examine the microstructure and detect ASR products. EDS analysis was also carried out to investigate the chemical composition of the ASR gel, including the reaction products within aggregate cracks, air voids, recycled rubber aggregate, and the interfacial transition zone between the RRA and cement paste.

A summary of the experimental program, including all test methods, key parameters, and their respective purposes, is provided in Table 3.

Table 3 Overview of experimental program and test methods

No	Test/analysis	Material/specimen	Standard/method	Key parameters	Purpose
1	NaOH treatment of RRA	Recycled rubber aggregate (0.5–1.0 mm)	Laboratory procedure	1 M NaOH, 30 min; drying at 20 °C or 80 °C	Simulation of alkaline exposure and surface modification
2	XRD analysis	Untreated and treated RRA	Bruker D8 DISCOVER	$2\theta = 5$–$65°$, step 0.02°, 1 s/step	Identification of crystalline phases and chemical stability
3	TGA analysis	Untreated and treated RRA	Perkin Elmer TGA 800	RT–800 °C, 10 °C/min, N_2 atmosphere	Evaluation of thermal stability and degradation behaviour
4	ATR-FTIR analysis	Untreated and treated RRA	Spectrum Two	400–4000 cm^{-1}	Detection of functional groups and surface oxidation
5	Flexural strength	Mortar prisms ($40 \times 40 \times 160$ mm^3)	EN 196–1	3-point bending, 28 days curing	Determination of tensile strength
6	Compressive strength	Mortar halves after bending	EN 196–1	Load to failure, 28 days curing	Determination of compressive strength
7	ASR expansion (AMBT)	Mortar bars ($25 \times 25 \times 285$ mm^3)	RILEM AAR-2	1 M NaOH, 80 °C, 28 days	Evaluation of ASR susceptibility and mitigation
8	SEM–EDS analysis	Post-mortem analysis, Mortar fragments after ASR test	SEM–EDS	15–20 kV, polished, carbon-coated, EDS point analysis	Microstructure and crack development. Chemical composition of reaction products

4 Results

As Fig. 2 shows, the XRD analysis of recycled rubber granulate revealed the presence of crystalline phases including zinc oxide and calcite, along with a broad amorphous background attributed to the organic components of the rubber, such as carbon black and the vulcanized polymer matrix. The comparison of untreated samples and those treated with 1 M NaOH at 20 °C and 80 °C showed no significant changes in peak positions or intensities, indicating that ZnO remained chemically stable under alkaline conditions.

The results on the thermogravimetric analyses presented in Fig. 3 revealed that all RRA specimens underwent major mass loss within the range 300–500 °C, corresponding to the decomposition of the polymeric matrix and carbonaceous phases. The weight loss % in this temperature range is characteristic to the thermal degradation of vulcanized rubber, corresponding to the breakdown of polyisoprene chains [24]. The weight (%) curves indicate that untreated RRA experienced the greatest overall mass loss, while NaOH-treated specimens at 80 °C produced the largest residue, suggesting improved thermal stability. The differences in the weight loss % in the alkali-treated specimens can be attributed to the removal of low-molecular-weight organic compounds and surface impurities during NaOH treatment.

In parallel, the DTG curves show that NaOH-treated specimens exhibit sharper and more distinct degradation peaks in the range 350–500 °C, with lower weight loss in the initial range between 250 and 300 °C, reflecting accelerated decomposition processes compared to the gradual profile of untreated RRA. This behavior suggests that alkaline treatment modifies the rubber network structure, likely through partial devulcanization or hydrolysis of sulphur crosslinks, resulting in a more homogeneous degradation pathway. No significant changes were observed below 120 °C, apart from negligible DTG signals associated with traces of surface-adsorbed moisture. Above 600 °C, additional weight of the specimen changes may be attributed to the further degradation of residual organics and mineral fillers, including the degradation of carbon black [25].

Figure 4 presents the FTIR spectra of recycled rubber aggregate in three conditions: untreated, treated with 1 M NaOH at 20 °C, and treated with 1 M NaOH at 80 °C. The analysis reveals distinct chemical changes of the rubber surface as a result of alkaline treatment, with temperature playing a significant role in the extent of alteration. All spectra show characteristic bands attributed to the polymeric components of vulcanized rubber, including:

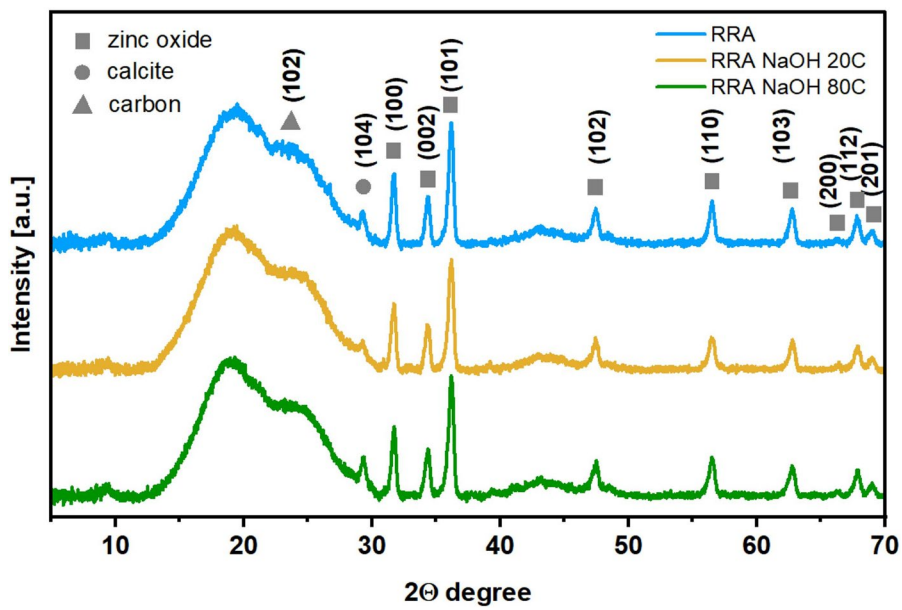

Fig. 2 XRD patterns of recycled rubber granulate untreated and treated with 1 M NaOH at 20 °C and 80 °C

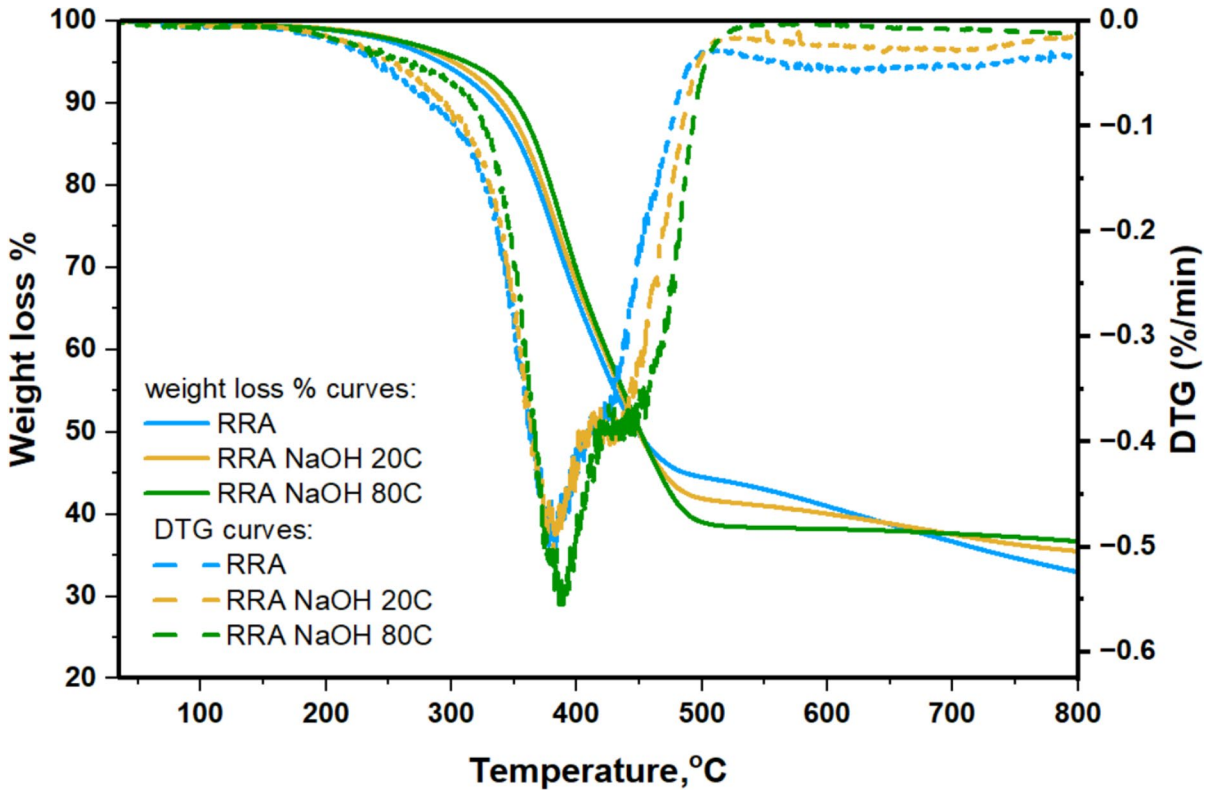

Fig. 3 TGA-DTG curves of recycled rubber granulate untreated and treated with 1 M NaOH at 20 °C and 80 °C

Fig. 4 The IR spectra of recycled rubber aggregate RRA untreated and treated with 1 M NaOH at 20 °C and at 80 °C

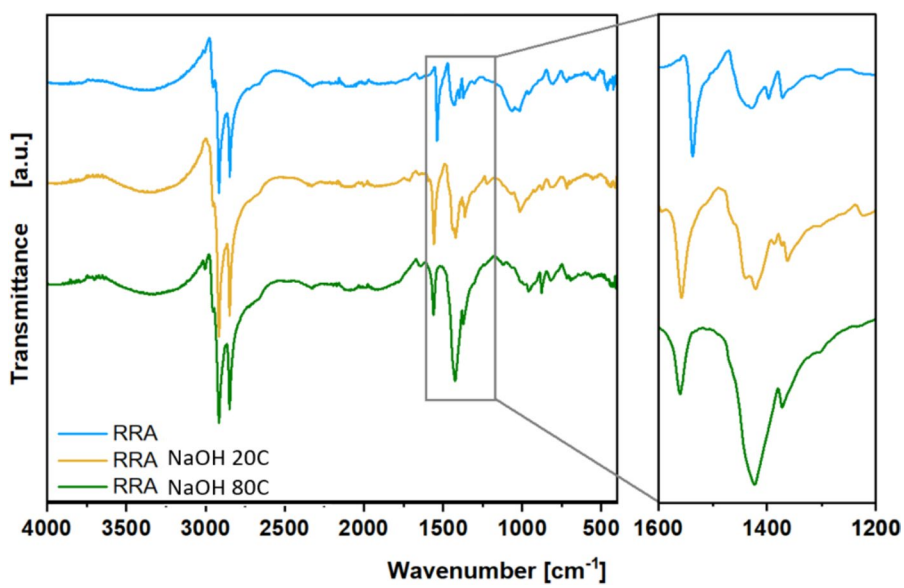

- broad band near 3350 cm^{-1}, corresponding to O–H stretching vibrations, which became more pronounced after NaOH treatment, indicating the formation of hydroxyl groups in the after the alkali treatment, while the presence of minor band around 1640 cm^{-1} can be attributed to the presence of water traces onto the surface,
- bands around 2900 cm^{-1}, associated with C–H stretching in unsaturated aliphatic chains in the polyisoprene, where the changes in the intensity in treated samples, particularly at 80 °C can suggest partial degradation of the polymeric structure, possibly surface of the RRA,
- bands in the range of 1000–1600 cm^{-1}, corresponding to functional groups such as C–C, C=C, C–O, and C–S. The changes in the band shape after the alkali treatment at 80 °C treatment, can be attributed to the chemical degradation of the rubber specimens through the partial oxidation or hydrolysis of rubber ingredients.
- bands in the 700 cm^{-1} and 872 cm^{-1} can be ascribed to the –C=C–H out of plane stretching, while bands located in the range 430–469 cm^{-1} and 562 cm^{-1} are characteristic to the –S–S– stretching vibrations in the vulcanized rubber [26, 27]. At the same time the bands located at 562 cm^{-1} and 700 cm^{-1} are characteristic of the Zn–O vibrations in the mineral filler [28].

The influence of recycled rubber aggregate on the mechanical properties of mortars is illustrated in Fig. 5, where both compressive strength f_c (Fig. 5a) and flexural strength f_t (Fig. 5b) exhibited an evident decreasing trend with RRA content. For mortars prepared with moderately reactive sand (S1), the reference mix without RRA (S1-M-0) showed the highest f_c and f_t. The introduction of 15% RRA (S1-M-15) led to a reduction of 12.4% in compressive strength and of 9.9% in flexural strength when compared to the reference specimen. When the RRA content was increased to 30% (S1-M-30), the compressive and flexural strength further decreased of 24.1% and 19.8%, respectively.

Similarly, for mortars made with highly reactive sand S2, the compressive strength decreased with respect to S2-M-0 mixture by 11.1% and 22.8% for 15% (S2- M-15) and 30% (S2-M-30) of RRA replacements, respectively. The corresponding flexural strength reductions were 9.2% and 18.5% for S2-M-15 and S2-M-30, respectively. Concerning S2-M-30_S3 (where 30% of the sand S2 was replaced with the non-reactive sand S3) the values of f_c and f_t were 41.5 MPa and 7.8 MPa, respectively. As these values are more or less coincident with those of S1-M-0 and S2-M-0, it means that the reduction of strength is only due to the substitution of stone sand with rubber aggregate, and not on the type of stone aggregate.

The effectiveness of RRA in mitigating ASR, evaluated through accelerated mortar bar tests at 80 °C in 1 M NaOH, is shown in Fig. 6. In the S1 series (Fig. 6a), the control mortar (S1-A-0), the mortar with 15% of RRA (S1-A-15), and the mortar with

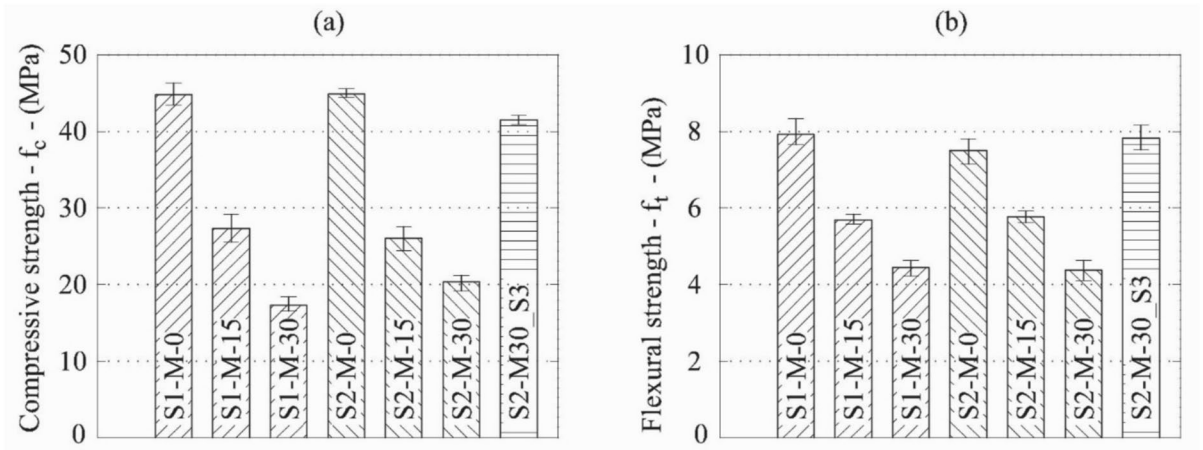

Fig. 5 The compressive (**a**) and flexural (**b**) strength results of M mortars after 28 days of curing

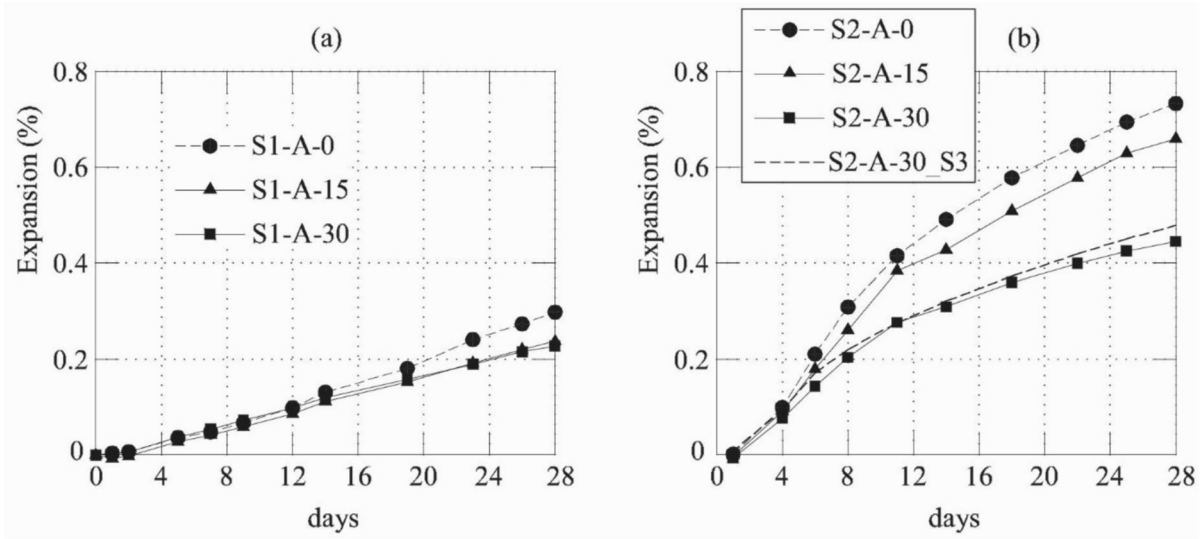

Fig. 6 Expansion of the tested mortars after 28 days of exposure to 1 M NaOH at 80 °C: (**a**) S1 series; (**b**) S2 series

30% RRA (S1-A-30) gave about the same expansion. More precisely, after 28 days, S1-A-0 exhibited the highest expansion (0.30%), whereas S1-A-15 and S1-A-30 showed an expansion of 0.23%. Thus, the presence of RRA provides a long-term mitigation in the case of moderately reactive sand.

In the S2 series (Fig. 6b), the effect of RRA was more pronounced. At 14 days, expansion dropped from 0.49% of the control mixture (S2-A-0) to 0.43% in the presence of 15% of RRA (S2-A-15), and to 0.33% with 30% of RRA (S2-A-30). After 28 days, these differences are more pronounced, because expansions reached ~ 0.73% for S2-A-0, ~ 0.66% for S2-A-15, and ~ 0.47% for S2-A-30.

The consistent reduction of expansion with increasing RRA content is evident when the performance of S2-A-30_S3 is compared with that of S2-A-30. Although the mixture S2-A-30 exhibited slightly lower expansion than S2-A-30_S3, the difference between these results is relatively small and may fall within experimental variability.

The microstructure of the mortars investigated in this project are illustrated with the SEM images reported in Figs. 7, 8, and 9. In the reference mortar without RRA (Fig. 7a), significant ASR-induced cracking and gel formation were observed around reactive aggregates. These cracks propagated throughout the matrix, indicating a severe ASR activity. Conversely, mortars with 15% RRA (Fig. 7b) displayed fewer cracks and reduced ASR gel formation: RRA disrupted reaction pathways and absorbed stresses, resulting into an effective mitigation of ASR-induced damage. This is particularly true in the mortar S2-A-30 containing 30% recycled rubber aggregate (Fig. 7c), where no cracks were observed in the surrounding cementitious matrix. Although ASR-induced cracking occurs within the reactive aggregate (Fig. 8), the cracks appear to reach only the immediate vicinity of the aggregate–cement matrix interface, where ASR gel is also observed near rubber particles, but do not propagate further into the matrix (Fig. 9). This suggests that the presence of RRA may interfere with crack propagation at this stage.

Figure 8 shows the SEM morphology of the reference sample with highly reactive sand S2 (i.e., S2-A-0). The general view (Fig. 8a) reveals distinct cracks in the aggregate grains and at the interface between cement paste and sand particles, with the presence of an expansive ASR gel. Moreover, EDS analysis (Fig. 8b), confirms the presence of Si and Na in the specimen S2-A-0, resulting from the silica- and alkali-rich ASR products concentrated around the aggregate surface and inside the cracks. A clear boundary can also be observed between the aggregate grain and the alkali–silica reaction products. Both SEM image and the EDS spectra show the different composition in the regions marked as (1) and (2) in Fig. 7b-c.

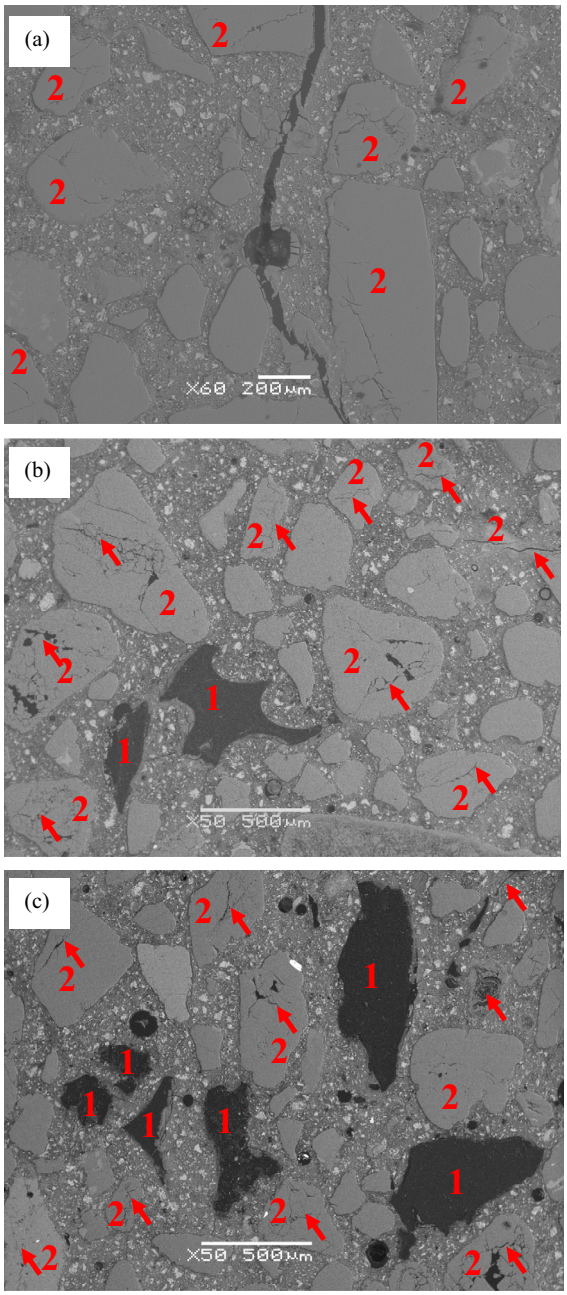

Fig. 7 SEM microstructure of mortars after the ASR test on polished surfaces, using highly reactive sand S2: (**a**) reference mortar S2-M-0; (**b**) mortar S2-M-15; and (**c**) mortar S2-M-30 (1—recycled rubber aggregate, 2—cracked aggregate grain)

Figure 9 presents the SEM microstructure of the contact zone between the cement matrix and recycled rubber aggregate in the mortar S2-A_30, incorporating 30% of RRA and highly reactive sand S2. The general view (Fig. 9a) reveals a well-preserved interface and an effective stress mitigation provided by the elastic RRA, with no visible cracks extending from the aggregate into the surrounding matrix. The detailed image with EDS line analysis (Fig. 9b) highlights a distinct interfacial zone, approximately $10 \div 15$ µm wide, characterized by altered microstructure and chemical composition of both rubber particle and cement paste. The EDS line scan showed an increased concentration of carbon within the rubber grain and a gradual transition to higher calcium and silicon contents in the cement paste, consistent with the presence of calcium silicate hydrate phases. A localized increase in sulphur was also observed near the interface, suggesting potential incorporation of sulphur-containing compounds, likely from the vulcanized rubber.

Complementary to the SEM analyses, the thermal studies with TGA were performed revealing clear differences in the thermal behaviour between RRA containing mortars after exposure in alkali media for 28 days. As can be seen in Fig. 10 all specimens exhibit an initial weight loss up to 100 °C that can relate to the evaporation of water that was adsorbed in the specimens or possibly dehydration of C-S–H, or ettringite [29]. The RRA-modified specimens show more intensive peaks in this region, which can be associated to the more intensive moisture retention from pores in the RRA-modified mortars compared to the bare mortar. Following region in the thermograms is mainly attributed to the portlandite decomposition (about 450 °C), while specimens S2-A-15 and S2-A-30 reveal additional peak around 380 °C that comes from the RRA degradation. Compared to the thermal studies for bare RRA specimens the decomposition of RRA in mortars occurs in 10 °C lower temperature for the catalytic effect of minerals [30]. Subsequent peaks located around 700 °C are attributed to the decarbonation of the calcium carbonate in the specimens. The RRA-modified specimens exhibit noticeable changes in peak shape and intensity, indicating that the incorporation of RRA affects the carbonation behaviour and microstructural morphology of the mortars. The sharp peaks in the S2-A-15 and S2-A-30 secimens above 500 °C can come from the granules disassembling for the non-homogeneous grains size in the grinded specimens.

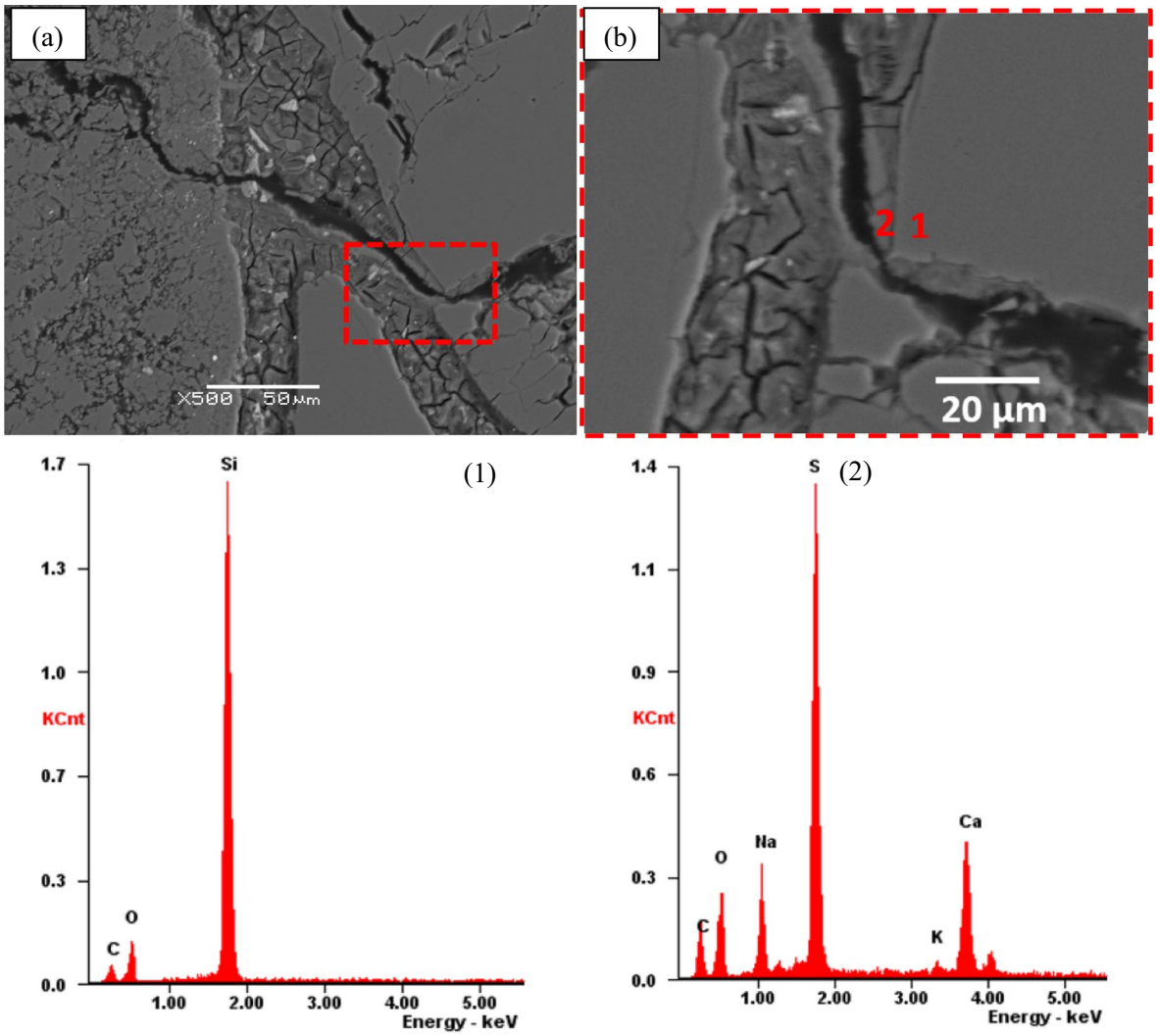

Fig. 8 SEM microstructure of the contact zone between cement matrix and aggregate affected by ASR in the reference mortar S2-A-0: (**a**) general views; (**b**) detailed image with EDS spectra

5 Discussion

The mechanical strength data revealed a consistent decrease in both compressive and flexural strength with increasing RRA content (see Fig. 5), which agrees with previous findings [10, 11, 31]. In particular, Gregori et al. [32] proposed a compressive strength reduction factor (SRF), defined as the ratio between the strength of rubberized and reference mortars, which can be bounded by the following empirical functions:

$$SRF = 0.247 + 0.753(1 - S)^{2.308} \quad (1a)$$

$$SRF = 0.001 + 0.999(1 - S)^{9.855} \quad (1b)$$

where, S = substitution rate of sand with rubber (in this paper, it is equal to 15% and 30%). As shown in Fig. 11a, the compressive SRF of the mortars M (Table 1) are exactly within the range bordered by Eqs. (1). Therefore, the main insight provided by Eqs. (1a–b) is not their predictive accuracy, but their

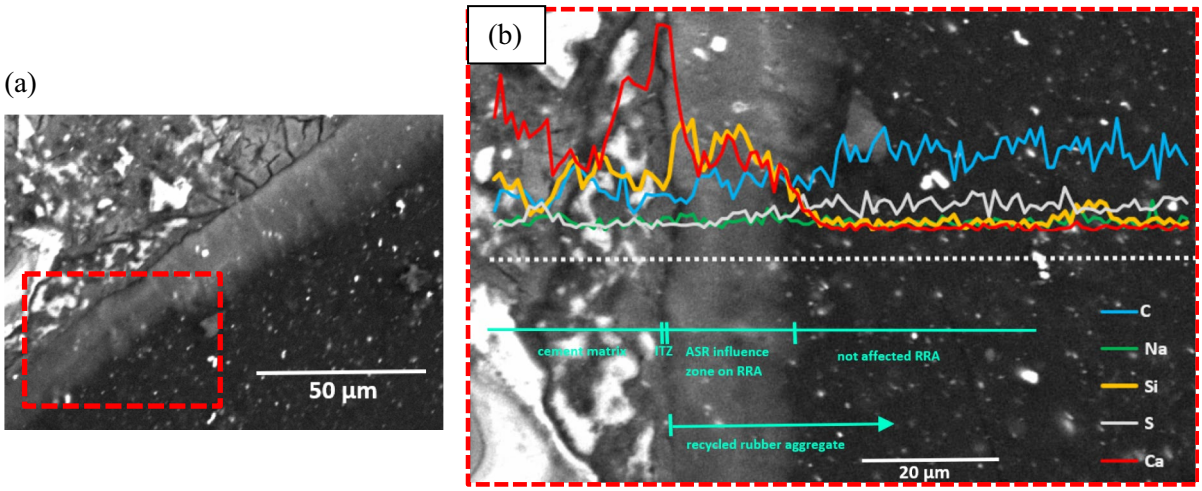

Fig. 9 SEM microstructure of the contact zone between the cement matrix and rubber aggregate affected by ASR in mortar S2-M-30 with polished surfaces: (**a**) general view; (**b**) detailed image with EDS line analysis

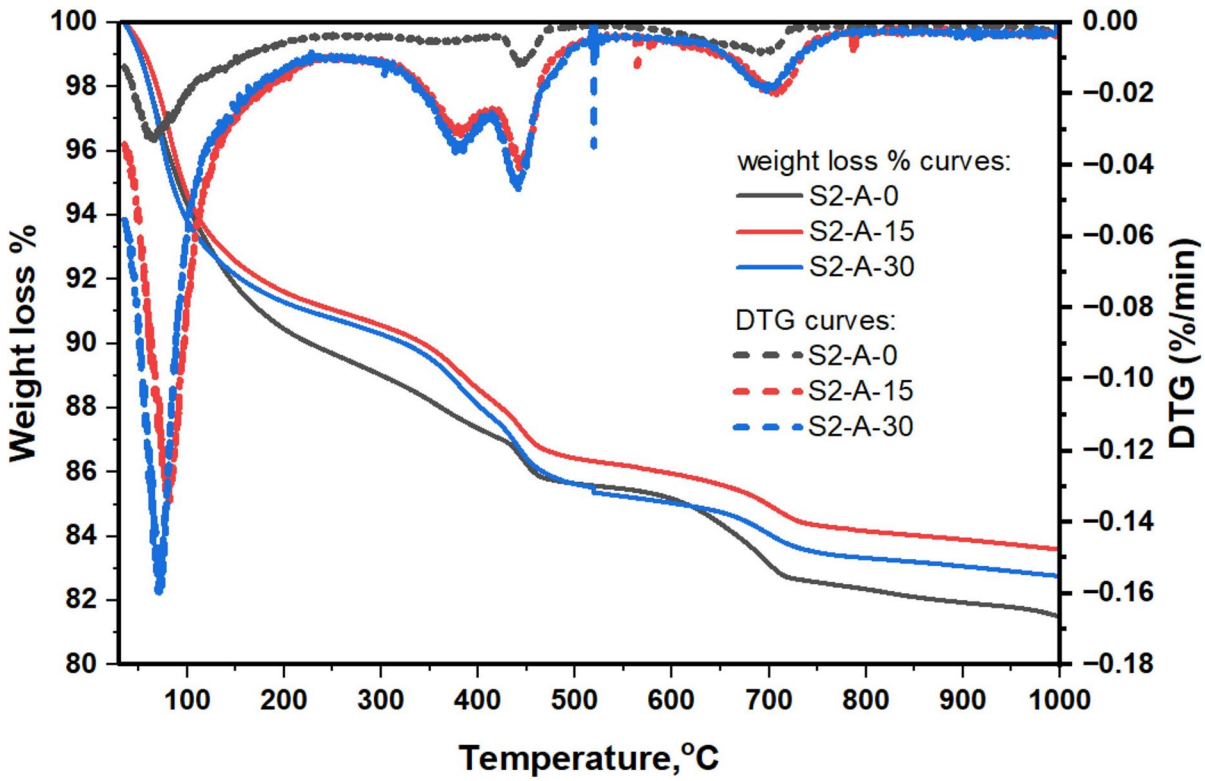

Fig. 10 TGA-DTG curves of S2-A-0, S2-A-15, and S2-A-30 after 28 days of NaOH treatment

ability to place the obtained results within a broader, previously established framework. Moreover, it is possible to observe that both mechanical performance and ASR mitigation trends can be described with similar empirical relationships.

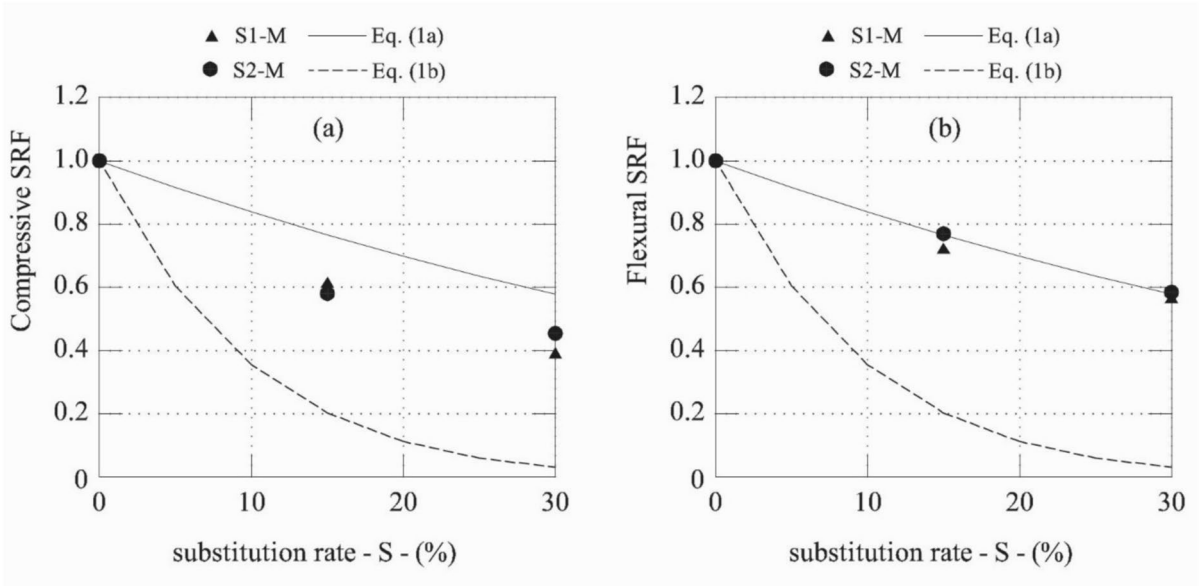

Fig. 11 Comparison between the strength reduction factors (SRF) experimentally measured in M mortars and those obtained by Gregori et al. [32]: (**a**) compressive strength; (**b**) flexural strength

When the same functions are compared with the flexural SRF values (Fig. 11b), only Eq. (1a) provides a reliable fit, suggesting that rubberized mortars retain a relatively higher flexural capacity compared to compressive strength. These losses of strength may be primarily attributed to the elastic nature of rubber, which deforms under load and reduces the stress transfer efficiency [33]. Moreover, a weakened and more porous interfacial transition zone, as well as an insufficient adhesion arising from the hydrophobicity of rubber particles [17, 33, 34], are also present. The ITZ observed in Fig. 7c does not exhibit the discontinuities typically reported in previous studies, which may be related to the different exposure conditions of the specimens and the apparent influence of NaOH on the near-surface behaviour of rubber. This conjecture is supported by the FTIR spectra of Fig. 4, which shows oxidation-related features indicative of increased rubber polarity. Also, the XRD results of Fig. 2 confirms that mineral fillers such as ZnO remains chemically stable under alkaline conditions [35].

All the previous findings suggest that NaOH exposure modifies the outer polymeric layer of RRA without altering its inorganic components and potentially enhancing local bonding with the cementitious matrix. Similar effects were reported by Mohammadi et al. [33], who demonstrated that NaOH treatment increases surface roughness and alters the interfacial chemistry of rubber, leading to temporary improvements in bonding with the cementitious matrix. For these reasons the flexural SRF is closer to the upper-bound of the range depicted in Fig. 10 than the compressive SRF.

Recent studies confirm that the incorporation of recycled rubber aggregate reduces compressive and flexural strength due to its low stiffness and weaker interfacial bonding [10, 11, 31]. This behaviour is also consistent with recent findings, where rubber incorporation leads to reduced compressive strength, but enhanced ductility and post-cracking performance [36]. However, this is accompanied by improved deformation capacity and crack resistance, as rubber particles act as flexible inclusions that redistribute internal stresses [37]. Regarding ASR mitigation, rubber aggregate has been shown to reduce expansion, depending on replacement level and particle characteristics [31]. This effect is attributed not only to dilution of reactive aggregates, but also to stress absorption and limited moisture transport within the microstructure [38]. Microstructural analyses further indicate that rubber modifies crack propagation at the aggregate–paste interface, contributing to reduced ASR-induced damage [39].

As shown in Fig. 6, the incorporation of recycled rubber aggregate in cement mortars significantly mitigated alkali-silica reaction, especially in mixes containing highly reactive aggregates S2 (Fig. 6b). Although both S2-A-30_S3 and S2-A-30 mixtures involved a 30% substitution of highly reactive aggregate with non-reactive materials, the difference in ASR-induced expansion between them is marginal and may lie within the bounds of experimental variability. Nevertheless, microstructural observations (Fig. 9) show the presence of a distinct interfacial transition zone between the cement matrix and the rubber particles, while FTIR analysis (Fig. 4) suggests that the rubber surface undergoes modification under alkaline conditions. These results imply that, in addition to the prevailing dilution effect, the incorporation of RRA may also provide a secondary contribution to ASR mitigation. Indeed, the elastic and hydrophobic characteristics of rubber [40, 41] promote stress redistribution and reducing internal moisture transport, respectively. Similar mechanisms have been reported in recent studies, where rubber inclusions were shown to act as stress-relieving phases, and capable of influencing transport properties and interfacial behaviour in cement-based composites [31, 42]. Moreover, rubber incorporation has been shown to influence permeability and moisture transport, which are critical factors in ASR development [37, 38, 42, 43]. These combined effects support the interpretation that ASR mitigation in rubberized systems is governed by a multi-mechanism process rather than dilution alone.

The hydrophobic nature of rubber has been associated with limited internal moisture mobility and disruptions in the aggregate–cement interface, conditions unfavourable for ASR development [17]. Although these effects were not examined directly in the present study, they are consistent with reduced permeability previously reported for rubberized systems [17]. This is also consistent with recent findings, where rubber substitution was shown to influence not only mechanical performance but also permeability characteristics of cement-based composites, further contributing to durability-related improvements [43]. Additionally, the elastic response of RRA may contribute to local stress dissipation and reduced crack formation during ASR gel expansion [42], in line with earlier observations of enhanced deformability and energy absorption in similar cement-based composites [12, 15].

Although SEM observations were performed on specimens exposed to 1 M NaOH, they provide insight into the potential mechanisms involved. As shown in Fig. 9, Ca and Si ions penetrated into the outer layer of the rubber particles, forming a transition zone that appeared more continuous than the sharply defined interface typically reported in the literature. While this phenomenon may be influenced by the alkaline exposure conditions, it suggests that a modified interfacial layer could contribute to more efficient stress redistribution under bending and, consequently, to ASR mitigation.

Accordingly, an expansion reduction factor (ERF) can be introduced and defined as the ratio between 28-day expansion of RRA mortars and that of the control mortars (S1-A-0 or S2-A-0):

$$\mathrm{ERF} = \frac{\text{expansion of the mortar}}{\text{expansion of the reference mortar}} \tag{2}$$

Interestingly, ERF values computed with Eq. (2) and reported in Fig. 12 is also close Eq. (1a), especially for mortars with low and high reactive aggregates. When the substitution rate is lower than 30%, both experimental and theoretical results show an almost linear decrement of ERF and SRF with the

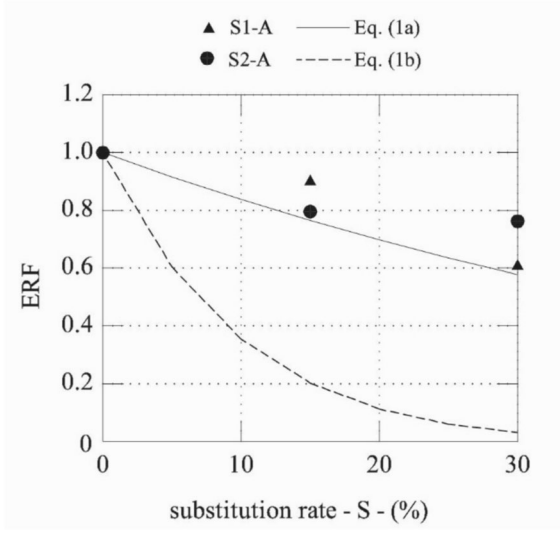

Fig. 12 Expansion reduction factors (ERF) versus Eq. (1a and 1b)

substitution rate *S*. This parallelism highlights that both flexural SRF and ERF are influenced by the same microstructural changes introduced by rubber, notably the formation of a ITZ and the stress-absorbing capacity of elastic inclusions.

It must be emphasized that Eqs. (1), derived from compressive strength data, can also be used to predict the reduction of flexural strength and of ASR expansion (Fig. 10b and Fig. 11). It is not a physical causality, but rather a general empirical correlation for different effects of rubber incorporation: in mechanics, SRF reflects reduced stress transfer and weaker ITZ, whereas in durability, ERF reflects stress relaxation and moisture control. Both these phenomena are due to the intrinsic properties of rubber [16, 33].

Although only few tests were performed herein, promising results arise from Fig. 10b and Fig. 11. Indeed, Eq. (1a) suggests the way to tailor cement-based systems containing both expansive aggregate and rubber from end-of-life tires. More specifically, it could not be necessary to perform mechanical and ASR expansion tests, but only one of these two tests could be sufficient to predict both the loss of flexural strength and the expansion rate. If other tests corroborate the results previously described, the use of Eq. (1a) will represent an interesting reason to incorporate RRA in mortars, and to foster circular economy practices in construction. Indeed, by repurposing waste tire rubber, not only landfill accumulation will be reduced, but also the reliance on natural aggregates will decrease, addressing critical environmental concerns. These sustainability benefits complement the technical advantages observed in mitigating ASR.

6 Conclusions

As a result, the use of recycled rubber aggregate as a partial replacement of fine sand in cement mortars affects both mechanical performance and ASR mitigation. In particular:

- RRA incorporation resulted in a reduction of compressive strength by up to 24.1% and flexural strength by up to 19.8% at 28 days, with higher substitution levels leading to greater strength losses.
- Despite this, a significant improvement in ASR resistance was observed. For highly reactive aggregates, expansion decreased from approximately 0.73% to 0.47%, corresponding to a reduction of up to 33%.
- Microstructural analyses showed that RRA creates a more continuous and flexible interfacial transition zone (≈ 10–15 μm), limiting crack propagation and reducing ASR-related damage.
- The mitigation effect is primarily attributed to the dilution of reactive aggregates, while the stress-absorbing capacity and hydrophobic nature of rubber may provide an additional, secondary contribution.
- A predictive relationship between the strength reduction factor (SRF) and expansion reduction factor (ERF) was proposed, enabling estimation of the required rubber content for ASR mitigation.

The study was conducted on mortar specimens under accelerated laboratory conditions, which may not fully represent long-term behaviour in concrete structures. Further research activities should focus not only on corroborating the results on mortars, but also on the long-term durability of full-scale concrete systems, in order to validate the applicability of RRA in practical engineering applications.

Acknowledgements The research presented in this article was funded by the European Commission under the HORIZON EUROPE project entitled “SMILE CITY-Sustainable materials for innovative low-emission applications in a circular city”, GA 101135406. M.O. would like the thank Paulina Pietrzyk-Thel and Adrianna Nowak for technical support, and prof. Michael Giersig for providing access to the laboratory facilities.

Author contributions Daria Jóźwiak-Niedźwiedzka: Conceptualization, Resources, Investigation, Funding acquisition, Formal analysis, Data curation, Supervision, Writing – original draft, Writing – review & editing. Dominik Nowicki: Investigation, Writing – review & editing. Piotr Denis: Investigation, Writing – review & editing. Magdalena Osial: Investigation, Writing – original draft, Writing – review & editing. Alessandro P. Fantilli: Resources, Funding acquisition, Formal analysis, Supervision, writing – original draft, Writing – review & editing.

Funding HORIZON EUROPE Climate, Energy and Mobility, GA 101135406, Daria Jozwiak-Niedzwiedzka, GA 101135406, Dominik Nowicki, GA 101135406, Alessandro Fantilli

Data availability Data will be made available on request.

Declarations

Competing interest The authors declare that they have no known competing financial interests or personal relationships that could have appeared to influence the work reported in this paper.

References

1. Thomas BS, Gupta RC (2016) A comprehensive review on the applications of waste tire rubber in cement concrete. Renew Sustain Energy Rev 54:1323–1333. https://doi.org/10.1016/j.rser.2015.10.092
2. Federal Highway Administration Research and Technology (2016) User guidelines for waste and by-product materials in pavement construction. Publication Number: FHWA-RD-97-148
3. EuRIC (2026) Harmonised end-of-waste criteria: a key step to strengthening Europe's tyre recycling market. https://tyreseurope.org/wp-content/uploads/2026/02/Recycling-Europe_Tyres-Europe-Joint-Position-Harmonised-EoW-criteria.pdf
4. Bravo M, de Brito J (2012) Concrete made with used tyre aggregate: durability-related performance. J Clean Prod 25:42–50. https://doi.org/10.1016/j.jclepro.2011.11.066
5. Muñoz-Sánchez B, Arévalo-Caballero MJ, Pacheco-Menor MC (2017) Influence of acetic acid and calcium hydroxide treatments of rubber waste on the properties of rubberized mortars. Mater Struct 50:75. https://doi.org/10.1617/s11527-016-0912-7
6. Passarini F, Ciacci L, Santini A et al (2012) Auto shredder residue LCA: implications of ASR composition evolution. J Clean Prod 23:28–36. https://doi.org/10.1016/j.jclepro.2011.10.028
7. Shu X, Huang B (2014) Recycling of waste tire rubber in asphalt and portland cement concrete: an overview. Constr Build Mater 67:217–224. https://doi.org/10.1016/j.conbuildmat.2013.11.027
8. Mohseni E, Koushkbaghi M (2023) Recycling of landfill waste tyre in construction materials: durability of concrete made with chipped rubber. Constr Build Mater 409:134114. https://doi.org/10.1016/j.conbuildmat.2023.134114
9. Atef M, Bassioni G, Azab N, Abdellatif MH (2021) Assessment of cement replacement with fine recycled rubber particles in sustainable cementitious composites. J Mech Behav Mater 30:59–65. https://doi.org/10.1515/jmbm-2021-0007
10. Huang W, Huang X, Xing Q, Zhou Z (2020) Strength reduction factor of crumb rubber as fine aggregate replacement in concrete. J Build Eng 32:101346. https://doi.org/10.1016/j.jobe.2020.101346
11. Li Y, Zhang S, Wang R, Dang F (2019) Potential use of waste tire rubber as aggregate in cement concrete—a comprehensive review. Constr Build Mater 225:1183–1201. https://doi.org/10.1016/j.conbuildmat.2019.07.198
12. Turatsinze A, Bonnet S, Granju J-L (2007) Potential of rubber aggregates to modify properties of cement based-mortars: improvement in cracking shrinkage resistance. Constr Build Mater 21:176–181. https://doi.org/10.1016/j.conbuildmat.2005.06.036
13. Hassanli R, Youssf O, Mills JE (2017) Experimental investigations of reinforced rubberized concrete structural members. J Build Eng 10:149–165. https://doi.org/10.1016/j.jobe.2017.03.006
14. Noaman AT, Abu Bakar BH, Akil HMd (2016) Experimental investigation on compression toughness of rubberized steel fibre concrete. Constr Build Mater 115:163–170. https://doi.org/10.1016/j.conbuildmat.2016.04.022
15. Ling TC, Nor HM, Lim SK (2010) Using recycled waste tyres in concrete paving blocks. Proc Inst Civ Eng Waste Resour Manag 163:37–45. https://doi.org/10.1680/warm.2010.163.1.37
16. Zhang D, Li H, Tu H, Weng Y (2022) Investigation on the quasi-static mechanical properties and dynamic compressive behaviors of ultra-high performance concrete with crumbed rubber powders. Mater Struct 55:104. https://doi.org/10.1617/s11527-022-01904-0
17. Wang J, Guo Z, Yuan Q et al (2020) Effects of ages on the ITZ microstructure of crumb rubber concrete. Constr Build Mater 254:119329. https://doi.org/10.1016/j.conbuildmat.2020.119329
18. Afshinnia K, Poursaee A (2015) The influence of waste crumb rubber in reducing the alkali–silica reaction in mortar bars. J Build Eng 4:231–236. https://doi.org/10.1016/j.jobe.2015.10.002
19. Abbas S, Ahmed A, Waheed A et al (2022) Recycled untreated rubber waste for controlling the alkali–silica reaction in concrete. Materials (Basel) 15:3584. https://doi.org/10.3390/ma15103584
20. Jóźwiak-Niedźwiedzka D, Antolik A, Dziedzic K, Lisowski P (2022) Potential alkaline reactivity of sands from domestic deposits. Roads Bridges Drogi Mosty 21:253–271. https://doi.org/10.7409/rabdim.022.015
21. AASHTO R 80-17 (2018) Standard practice for determining the reactivity of concrete aggregates and selecting appropriate measures for preventing deleterious expansion in new concrete construction, pp 1–25
22. PN-EN 196-1 (2016) Methods of testing cement—determination of strength, pp 1–33

23. Nixon JP, Sims I (2016) RILEM recommended test Method: AAR-2—Detection of potential alkali-reactivity—accelerated mortar-bar test method for aggregates. In: Nixon P (ed) RILEM Recommendations for the prevention of damage by alkali-aggregate reactions in new concrete structures, pp181
24. Bolloju S, Chang Y-L, Sharma SU et al (2022) Vulcanized polyisoprene-graft-maleic anhydride as an efficient binder for silicon anodes in lithium-ion batteries. Electrochim Acta 419:140390. https://doi.org/10.1016/j.electacta.2022.140390
25. Karabork F, Pehlivan E, Akdemir A (2014) Characterization of styrene butadiene rubber and microwave devulcanized ground tire rubber composites. J Polym Eng 34:543–554. https://doi.org/10.1515/polyeng-2013-0330
26. Colom X, Faliq A, Formela K, Cañavate J (2016) FTIR spectroscopic and thermogravimetric characterization of ground tyre rubber devulcanized by microwave treatment. Polym Test 52:200–208. https://doi.org/10.1016/j.polymertesting.2016.04.020
27. Xu F, Wang B, Yang D et al (2018) TG-FTIR and Py-GC/MS study on pyrolysis mechanism and products distribution of waste bicycle tire. Energy Convers Manag 175:288–297. https://doi.org/10.1016/j.enconman.2018.09.013
28. Masud RA, Islam MdS, Haque P et al (2020) Preparation of novel chitosan/poly (ethylene glycol)/ZnO bionanocomposite for wound healing application: effect of gentamicin loading. Materialia (Oxf) 12:100785. https://doi.org/10.1016/j.mtla.2020.100785
29. Ramanathan S, Halee B, Suraneni P (2020) Effect of calcium sulfoaluminate cement prehydration on hydration and strength gain of calcium sulfoaluminate cement-ordinary portland cement mixtures. Cem Concr Compos 112:103694. https://doi.org/10.1016/j.cemconcomp.2020.103694
30. Wang K, Shan T, Li B et al (2024) Study on pyrolysis characteristics, kinetics and thermodynamics of waste tires catalytic pyrolysis with low-cost catalysts. Fuel 356:129644. https://doi.org/10.1016/j.fuel.2023.129644
31. Kandil U, Bulut HA (2024) The effect of different proportions of waste rubber substitution on alkali-silica reaction and mechanical properties in mortars. Sakarya Univ J Sci 28:371–380. https://doi.org/10.16984/saufenbilder.1381564
32. Gregori A, Castoro C, Marano GC, Greco R (2019) Strength reduction factor of concrete with recycled rubber aggregates from tires. J Mater Civ Eng. https://doi.org/10.1061/(ASCE)MT.1943-5533.0002783
33. Mohammadi I, Khabbaz H, Vessalas K (2016) Enhancing mechanical performance of rubberised concrete pavements with sodium hydroxide treatment. Mater Struct 49:813–827. https://doi.org/10.1617/s11527-015-0540-7
34. Amiri M, Hatami F, Golafshani EM (2021) Evaluating the synergic effect of waste rubber powder and recycled concrete aggregate on mechanical properties and durability of concrete. Case Stud Constr Mater 15:e00639. https://doi.org/10.1016/j.cscm.2021.e00639
35. Jalal M, Nassir N, Jalal H (2019) Waste tire rubber and pozzolans in concrete: a trade-off between cleaner production and mechanical properties in a greener concrete. J Clean Prod 238:117882. https://doi.org/10.1016/j.jclepro.2019.117882
36. Mahato SK, Das SK, Biswas SK (2026) Investigating the potential of crumb rubber as fine aggregate replacement in sustainable concrete, pp 373–384
37. Maduranga DHA, Appuhamy JMRS, Bandara WMKRTW, Kankanamge CE (2025) Alkali-silica reaction (ASR) and mitigation methods for addressing the negative durable impact in glass-mix concrete: a comprehensive review. Engineer J Inst Eng Sri Lanka 58:67–81. https://doi.org/10.4038/engineer.v58i3.7705
38. Offei I, Guo A, Sun Z et al (2023) Preventing ASR-induced deteriorations with hydrophobic aggregates-a feasibility study. Constr Build Mater 394:132277. https://doi.org/10.1016/j.conbuildmat.2023.132277
39. Hasar UC, Korkmaz H, Nayyeri V (2025) Monitoring of alkali–silica-reaction (ASR) in cementitious concretes by microwave non-resonant waveguide measurements. Sci Rep 15:39769. https://doi.org/10.1038/s41598-025-23432-x
40. Zhu Z, Tai C, Zhang Y, Lu Y (2025) Effects and mechanisms of green-modified waste rubber particles on the mechanical properties and durability of cement-based materials. J Build Eng 104:112237. https://doi.org/10.1016/j.jobe.2025.112237
41. Momotaz H, Rahman MM, Karim MR et al (2023) Properties of the interfacial transition zone in rubberised concrete—an investigation using nano-indentation and EDS analysis. J Build Eng 77:107405. https://doi.org/10.1016/j.jobe.2023.107405
42. Zhang L, Feng M, Liu B et al (2024) Multi-scale study on the crack resistance and energy dissipation mechanism of modified rubberized concrete. Constr Build Mater 457:139448. https://doi.org/10.1016/j.conbuildmat.2024.139448
43. Mei X, Zeng J, Cui Z et al (2026) Influence of rubber substitution rate and cement content on the mechanical and permeability performance of high-content rubberized sand concrete. J Build Eng 120:115469. https://doi.org/10.1016/j.jobe.2026.115469